PERGAMON International Journal of Non-Linear Mechanics 34 (1999) 1047–1059

INTERNATIONAL JOURNAL OF
NON-LINEAR
MECHANICS

Sequences of orbits and the boundaries of the basin of attraction for two double heteroclinic orbits

Richard Haberman[a], Richard Rand[b,*]

[a]*Department of Mathematics, Southern Methodist University, Dallas, TX 75275, USA*
[b]*Department of Theoretical and Applied Mechanics, Cornell University, Ithaca, NY 14853, USA*

Received 8 August 1998

Abstract

The boundaries of the basin of attraction are usually assumed to be rather elementary for Hamiltonian systems with autonomous perturbations. In the case of one saddle point, the sequences of orbits before capture are unique for each basin. However, we show that for two saddle points each with double heteroclinic orbits, there is an infinite number of different sequences of nearly homoclinic orbits before capture depending on the four heteroclinic parameters. The probabilities of capture are independent of the capture sequence.

Keywords: Hamiltonian; Perturbation; Dissipation; Capture; Homoclinic; Heteroclinic; Melnikov

1. Introduction

Numerous physical problems satisfy two-dimensional Hamiltonian systems or other conservative systems characterized by regions of periodic solutions. We study systems with periodic regions (surrounding a center) separated by heteroclinic or homoclinic orbits which connect unstable saddle points. Typical examples include dynamical systems describing various kinds of resonance. These include applications to attitude dynamics of dual-spin spacecraft [1–3] and orbital dynamics of tidally evolving natural satellites [4, 5]. Under small autonomous perturbations, the system is no longer conservative and solutions may slowly pass through the separatrix (homoclinic or heteroclinic orbits). Near the separatrix, the change in the Hamiltonian or energy from one saddle approach to the next may be approximated by a dissipation or Melnikov integral. Heteroclinic or homoclinic connections generically break, and solutions are captured into competing attractors (such as a stable spiral or a stable limit cycle). The boundaries of the basins of attraction (that is, the stable manifold of the saddle points) are thin and spiral-like for small perturbations. The probabilities of capture are the ratio of specific dissipation integrals as shown by Arnold [6] and Neishtadt [7]. Near the separatrix, Timofeev [8] suggested that the solution can be approximated by nearly homoclinic

* Corresponding author.

0020-7462/99/$ - see front matter
PII: S0020-7462(98)00075-4

orbits. Tennyson et al. [9] determined the jump in action during the slow passage through a separatrix by analyzing the large sequence of nearly homoclinic orbits. Bourland and Haberman [10] showed that the large sequence of nearly homoclinic orbits can be matched to the slowly varying non-linear oscillations before and after the slow passage through the separatrix. Under small dissipative and periodic perturbations, the amplitude of the periodic forcing may be used as a bifurcation parameter [11]. Stable and unstable subharmonic periodic solutions are created as the amplitude increases though the probability of capture into these is small. The smallest amplitude at which all subharmonic periodic solutions exist coincides with the amplitude at which chaos first occurs using the homoclinic Melnikov criteria for chaos. The subharmonic periodic solutions coalesce onto the homoclinic orbit. In chaos any sequence of nearly homoclinic orbits is possible. Under the simpler autonomous perturbation we consider here, usually there are only a small number of different sequences of nearly homoclinic orbits before capture. However, here we show that the topological structure of orbits may be quite complex even for a simple autonomously perturbed conservative system with two saddle points connected by double heteroclinic orbits. We show there can be an infinite number of different sequences of nearly heteroclinic orbits before capture for different values of the four heteroclinic dissipation integrals.

2. Perturbed Hamiltonian systems

Although we will not restrict our attention to perturbed Hamiltonian systems in this paper, we shall motivate this work by briefly reviewing the salient features of such systems:

$$\frac{\mathrm{d}q}{\mathrm{d}t} = \frac{\partial H}{\partial p} + \varepsilon f(q,p), \quad \frac{\mathrm{d}p}{\mathrm{d}t} = -\frac{\partial H}{\partial q} + \varepsilon g(q,p) \tag{1}$$

where $H(q,p)$ is the Hamiltonian and ε is a small parameter ($0 < \varepsilon \ll 1$). We assume the unperturbed problem ($\varepsilon = 0$) has at least one saddle point and at least one homoclinic orbit or heteroclinic orbit. For $0 < \varepsilon \ll 1$, there are solutions which are nearly homoclinic or nearly heteroclinic which we will analyze. Since

$$\mathrm{d}H/\mathrm{d}t = \varepsilon\left(f(q,p)\frac{\partial H}{\partial q} + g(q,p)\frac{\partial H}{\partial p}\right),$$

the change in the Hamiltonian from t_1 to t_2 is

$$\Delta H = \varepsilon\int_{t_1}^{t_2}\left(f(q,p)\frac{\partial H}{\partial q} + g(q,p)\frac{\partial H}{\partial p}\right)\mathrm{d}t.$$

Thus, the change in the Hamiltonian from one saddle approach to the next can be asymptotically approximated by

$$\Delta H \approx \varepsilon\int_{-\infty}^{\infty}\left(f(q,p)\frac{\partial H}{\partial q} + g(q,p)\frac{\partial H}{\partial p}\right)\mathrm{d}t,$$

where in this integral the solution is approximated by the unperturbed homoclinic orbit or heteroclinic orbit. For nearly homoclinic orbits the integral is a closed loop integral along the unperturbed homoclinic orbit while for nearly heteroclinic orbits the integral is a loop integral from one saddle point to another saddle point. These integrals are often referred to as homoclinic or heteroclinic Melnikov functions. We introduce a sign change

$$\Delta H \approx -D, \tag{2}$$

where

$$D = -\varepsilon\int_{-\infty}^{\infty}\left(f(q,p)\frac{\partial H}{\partial q} + g(q,p)\frac{\partial H}{\partial p}\right)\mathrm{d}t \tag{3}$$

where again the integral is to evaluated along the unperturbed homoclinic or heteroclinic orbit. We refer to this as a dissipation integral (since in physical problems often the change in energy is negative due to small damping). We will also use D to refer to the homoclinic or heteroclinic orbit itself.

In this paper, we use Eq. (2) but we do not assume that the change in the Hamiltonian is derived for a specific perturbation of the form defined by Eq. (1). Instead, we just assume there is a problem, perhaps different from Eq. (1), which gives rise to expression (2).

3. One saddle point with a double homoclinic orbit

Consider a system which before perturbation contains a saddle point and a homoclinic orbit (Fig. 1).

Without loss of generality, we assume H achieves a maximum at the center in Fig. 1 (denoted by a + sign) and we assume counterclockwise motion around the homoclinic orbit. Under perturbation, the saddle connection of Fig. 1 will in general break. Then depending on the sign of the dissipation integral D_1, the perturbed system may or may not exhibit an attractor (see Fig. 2).

An attractor occurs if $D_1 < 0$. In this case, if we take $H_{\text{saddle}} = 0$, then motions which reach the *entrance saddle approach* point P with energy H between 0 and $-D_1 > 0$, are captured by the attractor. Motions which arrive at P with energy larger than $-D_1$ pass around the capture boundary (which is the stable manifold of the saddle) and are not captured.

Consider next a more complicated system in which the unperturbed phase portrait consists of a saddle point accompanied by *two* homoclinic orbits (Fig. 3).

We assume clockwise motion at infinity. In this case there are two centers. We again assume that H achieves a maximum at the center closest to the saddle, and a minimum at the other center (respectively, denoted by a + and − sign). There are two dissipation integrals here, D_1 and D_2, each associated with one of the homoclinic orbits. As in Figs. 1 and 2, we again require $D_1 < 0$ in order that the region inside the smaller homoclinic orbit be attractive under perturbation. We also want the region between the two homoclinic orbits to be attractive. Here the relevant energy change is related to the sum $D_1 + D_2$, and since H is a minimum at the unperturbed center, the required condition is $D_1 + D_2 > 0$.

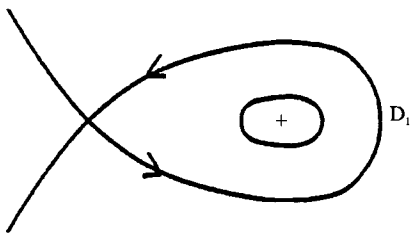

Fig. 1. Unperturbed system.

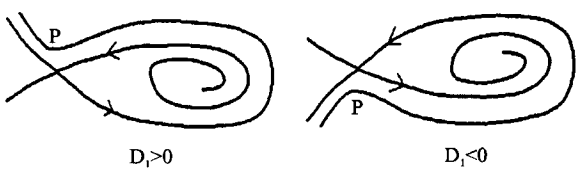

Fig. 2. An attractor occurs if $D_1 < 0$.

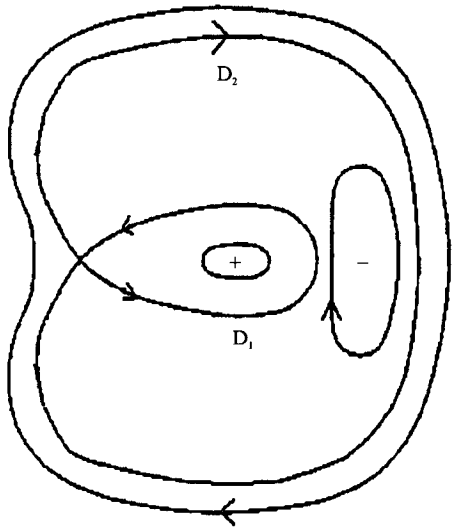

Fig. 3. Unperturbed system.

Note that the conditions $D_1 < 0$ and $D_1 + D_2 > 0$ require that $D_2 > 0$. If the energy at infinity is positive relative to $H_{\text{saddle}} = 0$, then $D_2 > 0$ causes motions coming from infinity to approach the two regions of attraction. Note also that one branch of the stable manifold (marked *a*) has energy D_2 at the entrance saddle approach point P, while the other branch of the stable manifold (marked *b*) has energy D_1 at the first saddle approach but energy $D_1 + D_2$ at the entrance saddle approach. Thus motions which reach the entrance saddle approach P with energy H between 0 and $D_1 + D_2 > 0$, are captured into the right capture region, while motions with energy at P between $D_1 + D_2 > 0$ and D_2 end up in the left capture region (Fig. 4). A motion reaching P with

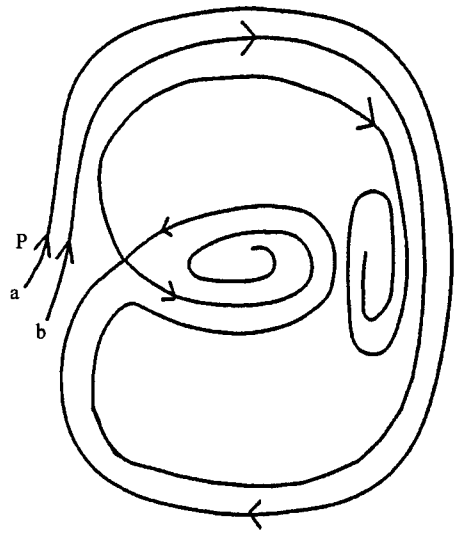

Fig. 4. Perturbed system for $D_1 < 0$, $D_1 + D_2 > 0$ (so that $D_2 > 0$). Trajectory a has approximate energy D_2 at entrance saddle approach P, while b has energy $D_1 + D_2$ there.

energy larger than D_2 misses being captured and makes an orbit encircling both capture regions. When it returns to the entrance saddle approach point P, however, it has lost energy $\Delta H \approx -D_2$. It continues to repeat this type of motion until its energy finally drops below D_2. Thus capture into the right capture region involves the sequence

$$D_2D_2D_2D_2...D_2D_2 : D_2D_1D_2D_1D_2...$$

while capture into the left capture region involves the sequence

$$D_2D_2D_2D_2...D_2D_2 : D_2D_1D_1D_1D_1....$$

(The colon in this sequence marks the entrance saddle approach point here and in the rest of this paper.) The probability of capture [7] into the right capture region is $(D_1 + D_2)/D_2$, while the probability of capture into the left capture region is $-D_1/D_2$.

Fig. 5 shows an unperturbed phase portrait which involves a saddle point and two homoclinic loops, but which is topologically distinct from that of Fig. 3. In this case we assume clockwise orbits at infinity and that both the left and right centers are

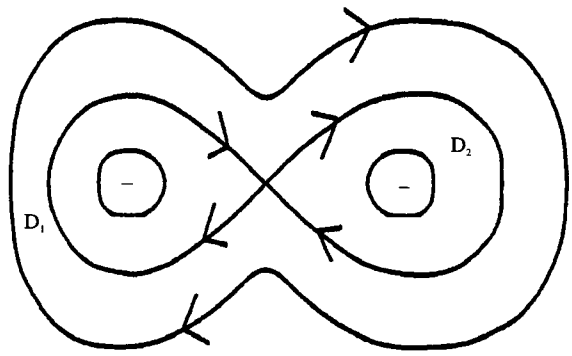

Fig. 5. Unperturbed system.

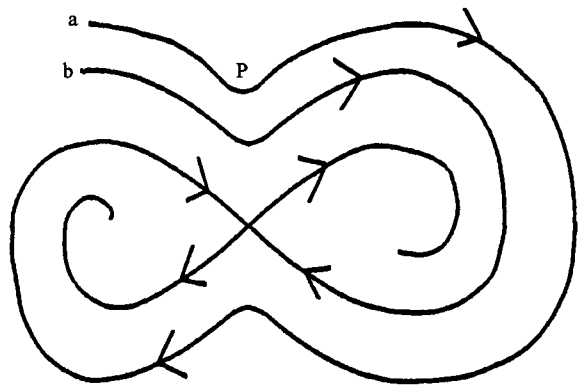

Fig. 6. Perturbed system for $D_1 > 0$ and $D_2 > 0$. Trajectory b has approximate energy D_2 at entrance saddle approach P, while a has energy $D_1 + D_2$ there.

local minima for H, i.e. potential wells. In order for both the left and right wells to be attractive, we require $D_1 > 0$ and $D_2 > 0$. These conditions give $D_1 + D_2 > 0$, so that if the energy at infinity is positive relative to $H_{\text{saddle}} = 0$, then motions coming from infinity will approach the two regions of attraction. See Fig. 6.

Note that one branch of the stable manifold (marked b) has energy D_2 at the entrance saddle approach point P, while the other branch of the stable manifold (marked a) has energy D_1 at the first saddle approach but energy $D_1 + D_2$ at the entrance saddle approach. Thus motions which reach the entrance saddle approach P with energy H between 0 and D_2, are captured into the right

well, while motions with energy at P between D_2 and $D_1 + D_2$ are captured into the left well. A motion reaching P with energy larger than $D_1 + D_2$ encircles both capture regions, losing energy $\Delta H \approx -(D_1 + D_2)$ each time around. It continues to repeat this type of motion until its energy finally drops below $D_1 + D_2$. Thus capture into the right well involves the sequence

$$D_2D_1D_2D_1...D_2D_1 : D_2D_2D_2D_2...$$

while capture into the left well involves the sequence

$$D_1D_2D_1D_2...D_2D_1 : D_2D_1D_1D_1D_1....$$

The probability of capture [7] into the right well is $D_2/(D_1 + D_2)$, while the probability of capture into the left well is $D_1/(D_1 + D_2)$.

4. Two saddle points with two double heteroclinic orbits

Fig. 7 shows an unperturbed phase portrait which involves two saddle points and four heteroclinic loops. Our interest in this work is to investigate the manner in which this phase portrait changes due to generic perturbation.

In this case, we assume (without loss of generality) that the motion is clockwise at infinity and that H is maximum at the middle center and minimum at the left and right centers. As in the previous two examples, the energy at infinity is assumed to be positive relative to the energy at the saddle points (and heteroclinic orbits) which we normalize to zero. Under small perturbation, the saddle points remain saddle points and the heteroclinic connections generically break.

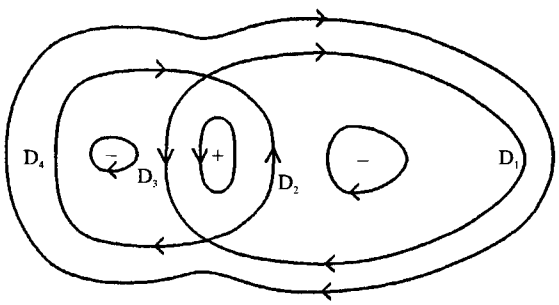

Fig. 7. Unperturbed system.

We shall be interested in the particular form of the perturbed phase portrait for given values of the dissipation integrals D_1, D_2, D_3, D_4. The case we investigate is the one in which all three regions become competing attractors. We shall refer to the left, right, and middle capture regions, respectively, as L, R and M in what follows. In order for the L to be an attractor under the perturbation, we require that $D_3 + D_4 > 0$, since the energy will then decrease from its zero value at the corresponding double heteroclinic orbit to the negative energy associated with being inside the left region. Similarly, R will be attractive if $D_1 + D_2 > 0$. M will be attractive if $D_2 + D_3 < 0$ since energy must increase for orbits to go from the zero energy of its corresponding heteroclinic orbit to the positive energy associated with the middle region. In summary, the three regions will all be competing attractors if

$$D_1 + D_2 > 0, \tag{4}$$

$$D_3 + D_4 > 0, \tag{5}$$

$$D_2 + D_3 < 0. \tag{6}$$

By adding Eqs. (4) and (5) we have

$$D_1 + D_2 + D_3 + D_4 > 0 \tag{7}$$

which with Eq. (6) implies that

$$D_1 + D_4 > 0. \tag{8}$$

This shows that motions coming from infinity must approach the three regions of attraction.

In the process of being captured, a given motion will undergo a sequence of types of nearly heteroclinic orbits, similar to the sequences of homoclinic orbits observed in the previous two examples. The possible sequences are determined by the relative values of the dissipation integrals D_i. We will show that a countable infinity of distinct capture sequences can occur.

As we will see, the sequence of types of nearly heteroclinic orbits is determined from the topology of the four branches of the stable manifold (two branches of the stable manifold of each of

two saddle points). Each saddle point gives rise to two capture regions, and hence there will be four thin bands corresponding to only three competing capture regions. One basin must split into two parts. The relative positions of these four branches of the stable manifold are computed using the change in energy from one saddle approach to the next.

Since $D_2 + D_3 < 0$, we analyze the three cases depending on the signs of D_2 and D_3:

Case I: $D_2 < 0$ and $D_3 < 0$,

Case II: $D_2 > 0$ and $D_3 < 0$,

Case III: $D_2 < 0$ and $D_3 > 0$.

Case I turns out to be rather simple with only one topological situation possible (as in problems with one saddle point), while cases II and III have an countably infinite number of topological situations possible. The probability of capture will be the same in all cases. Note that systems in which the original flow and its perturbations have left–right symmetry correspond to case I, since $D_4 = D_1$ and $D_3 = D_2$.

5. Case I: Unique topology

Case I is defined by $D_2 < 0$ and $D_3 < 0$. Eqs. (4) and (5) require that $D_1 > 0$ and $D_4 > 0$. In order to see what effect these constraints have on the topology of the stable manifold, we begin by following the four branches as they move backward in time from their respective saddle point to the first saddle approach, see Fig. 8. For example, in the case of the branch marked a, the requirement that $D_4 > 0$ causes H to increase as we move backward in time, thus causing branch a to move outside L. On the other hand, the condition $D_3 < 0$ causes branch b to move into L as we move backward in time. For convenience we will omit the phrase "backward in time" in what follows.

Note that branch a has reached the entrance saddle approach in Fig. 8 with energy $D_4 + D_1$. We continue to follow branches a, b, d as they evolve. For example, branch b, located inside L in Fig. 8, now moves close to heteroclinic connection D_4. Since $D_4 > 0$, H increases, and this tends to move branch b towards the outside of L. The net result of $D_3 < 0$ pushing b into L and $D_4 > 0$ pulling b out

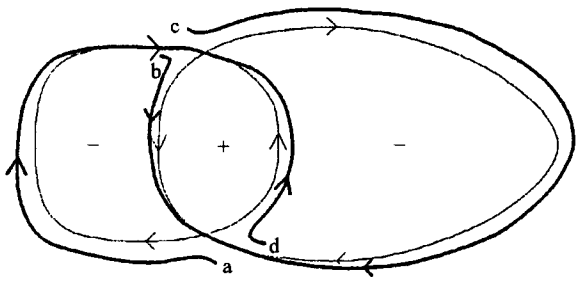

Fig. 8. Perturbed system, Case I: $D_2 < 0$, $D_3 < 0$, $D_1 > 0$, $D_4 > 0$. The energies at the first saddle approach of the four branches of the stable manifolds are: $a = D_4$, $b = D_3$, $c = D_1$, $d = D_2$. The unperturbed heteroclinic connections are shown as lighter lines.

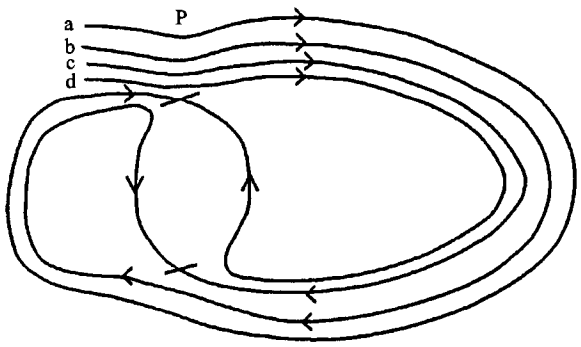

Fig. 9. Perturbed system, Case I: $D_2 < 0$, $D_3 < 0$, $D_1 > 0$, $D_4 > 0$. The energies at the entrance saddle approach P of the four branches of the stable manifolds are: $a = D_4 + D_1$, $b = D_3 + D_4 + D_1$, $c = D_1$, $d = D_2 + D_1$.

of L is determined by noting that $D_3 + D_4 > 0$ from Eq. (5), showing that b lies outside of L at its second saddle approach. Fig. 9 shows the continuation of this process, to the point where all four branches have been extended to the entrance saddle approach point P. From this figure we see that a motion which arrives at P with energy between 0 and $D_2 + D_1$ will approach R, while if its energy lies between $D_2 + D_1$ and D_1, it will approach M. If its energy lies between D_1 and $D_3 + D_4 + D_1$, it will approach L, and if its energy lies between $D_3 + D_4 + D_1$ and $D_4 + D_1$, it will approach M. If its energy is larger than $D_4 + D_1$ it misses the entrance saddle approach and circulates around the three capture regions, losing energy

$\Delta H \approx -(D_4 + D_1)$ each time around, until it eventually gets captured.

Note that M is approached in two ways giving rise to two different thin bands of orbits. From these considerations we see that the probability of capture into each of the capture regions is given by:

$$P(R) = \frac{D_1 + D_2}{D_1 + D_4} \tag{9}$$

$$P(L) = \frac{D_3 + D_4}{D_1 + D_4} \tag{10}$$

$$P(M) = \frac{-D_2}{D_1 + D_4} + \frac{-D_3}{D_1 + D_4} = \frac{-D_2 - D_3}{D_1 + D_4}. \tag{11}$$

The sequence of nearly heteroclinic orbits for solutions entering R is

$$D_1D_4D_1D_4...D_1D_4 : D_1D_2D_1D_2D_1D_2...,$$

while the sequence for solutions entering L is

$$D_1D_4D_1D_4...D_1D_4 : D_1D_4D_3D_4D_3... .$$

There are two possible sequences for M:

$$D_1D_4D_1D_4...D_1D_4 : D_1D_2D_3D_2D_3D_2D_3...$$

and

$$D_1D_4D_1D_4...D_1D_4 : D_1D_4D_3D_2D_3D_2D_3D_2....$$

6. Case II: Infinitely many topological situations

Case II is defined by $D_2 > 0$ and $D_3 < 0$. Eq. (5) requires that $D_4 > 0$. There is no restriction on the sign of D_1. This case will turn out to be more complicated than case I, and so we will consider the location of the four branches of the stable manifold individually. Consider first the branch of the stable manifold of the upper saddle point which begins by lying in the neighborhood of D_4. Since $D_4 > 0$, its first saddle approach occurs outside of L. Then it continues it journey by lying in the neighborhood of D_1. Since $D_4 + D_1 > 0$ from Eq. (8), this branch achieves the entrance saddle approach after these two nearly heteroclinic orbits, see a in Fig. 10.

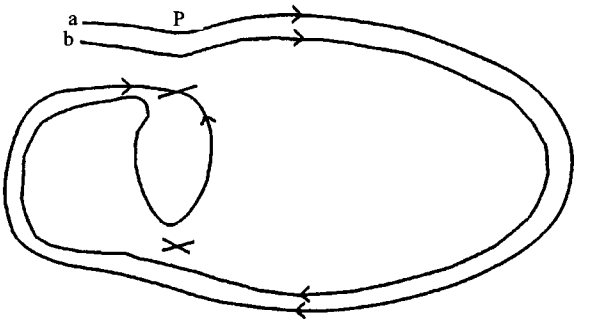

Fig. 10. Perturbed system, Case II: $D_2 > 0$, $D_3 < 0$, $D_4 > 0$. The energies at the entrance saddle approach P of the two branches of the stable manifold of the upper saddle point are: $a = D_4 + D_1$, $b = D_2 + D_3 + D_4 + D_1$.

Fig. 10 also shows the location of the second branch b of the stable manifold of the upper saddle. This one begins by lying in the neighborhood of D_2. Since $D_2 > 0$, its first saddle approach occurs inside of M. Then it follows D_3 around back towards the upper saddle point. From Eq. (6), $D_2 + D_3 < 0$ so that it lands outside of M and inside of L at its second saddle approach. It follows D_4 for its third saddle approach, which lies outside of L, M and R because $D_2 + D_3 + D_4 > 0$, which is deduced from the hypothesis that $D_2 > 0$ and Eq. (5). Finally it follows D_1 and achieves the entrance saddle approach in view of $D_2 + D_3 + D_4 + D_1 > 0$, which we see from Eqs. (4) and (5).

From Fig. 10 we also see that the probability of capture into M is

$$P(M) = \frac{-D_2 - D_3}{D_1 + D_4}, \tag{12}$$

which is the same as in case I. In addition, there is a unique sequence of orbits for capture into M:

$$D_1D_4D_1D_4...D_1D_4 : D_1D_4D_3D_2D_3D_2D_3D_2....$$

The boundary of the basin of attraction for M is rather simple, but we will show that the boundaries of the basins of attraction for L and R may wrap themselves around M an arbitrary number of times. This is because the two branches of the stable manifold of the lower saddle may be somewhat complicated.

6.1. Case II, continued: First branch of the stable manifold of the lower saddle point

Let us take the first branch of the stable manifold of the lower saddle point to be the one that begins with the nearly heteroclinic orbit which we have denoted D_1. If $D_1 > 0$, this branch of the stable manifold immediately achieves the entrance saddle approach with only one nearly heteroclinic orbit (see Fig. 11).

However, it is not necessary that $D_1 > 0$. If $D_1 < 0$ this branch will be more complicated than just one nearly heteroclinic orbit (and may be much more complicated). Specifically, if $D_1 < 0$, then this branch does not achieve the entrance saddle approach after one nearly heteroclinic orbit, but rather lies in region R. It then proceeds to follow in sequence orbits D_2, D_3, D_4 and then D_1 again. This conclusion is based on the following inequalities:

$D_1 + D_2 > 0$ from Eq. (4),

$D_1 + D_2 + D_3 < 0$ from Eq. (6) and $D_1 < 0$,

$D_1 + D_2 + D_3 + D_4 > 0$ from Eqs. (4) and (5).

Now on its final pass along D_1 it achieves the entrance saddle approach if $D_1 + D_2 + D_3 + D_4 + D_1 > 0$ (see Fig. 12), but it misses the entrance saddle approach and goes around again if $D_1 + D_2 + D_3 + D_4 + D_1 < 0$.

If $D_1 + D_2 + D_3 + D_4 + D_1 < 0$, the orbit once again proceeds to follow in sequence the heteroclinic orbits D_2, D_3, D_4 and then D_1 again. This conclusion is based on the following inequalities

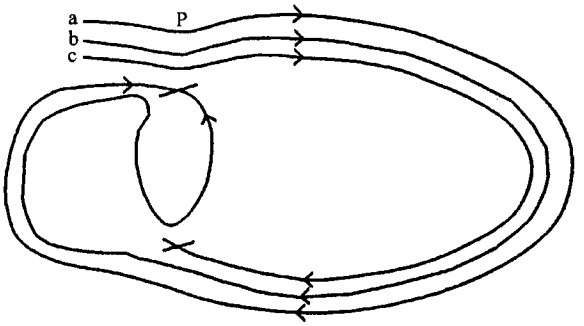

Fig. 11. Perturbed system, Case II: $D_2 > 0, D_3 < 0, D_4 > 0$, with $D_1 > 0$. The first branch of the lower saddle point, c, has been added to Fig. 10. Its energy at the entrance saddle approach P is $c = D_1$.

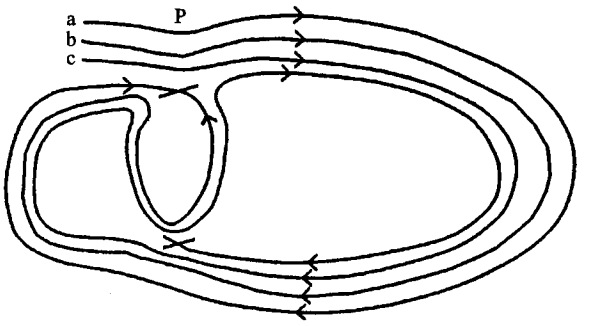

Fig. 12. Perturbed system, Case II: $D_2 > 0, D_3 < 0, D_4 > 0$, with $D_1 < 0$, but $D_1 + D_2 + D_3 + D_4 + D_1 > 0$. The first branch of the lower saddle point, c, has been added to Fig. 11. Its energy at the entrance saddle approach P is $c = D_1 + D_2 + D_3 + D_4 + D_1$. Cf. Fig. 11.

(where the parentheses have been added to aid in identification of quantities of known sign): $(D_1 + D_2) + (D_3 + D_4) + (D_1 + D_2) > 0$ from Eqs. (4) and (5); $(D_1 + D_2 + D_3 + D_4 + D_1) + (D_2 + D_3) < 0$ from Eq. (6) and the hypothesis $D_1 + D_2 + D_3 + D_4 + D_1 < 0, (D_1 + D_2) + (D_3 + D_4) + (D_1 + D_2) + (D_3 + D_4) > 0$ from Eqs. (4) and (5). Now on its final pass along D_1 it achieves the entrance saddle approach if $2(D_1 + D_2 + D_3 + D_4) + D_1 > 0$, but it misses the entrance saddle approach and goes around again if $2(D_1 + D_2 + D_3 + D_4) + D_1 < 0$.

This situation can be generalized as follows: If $D_1 < 0$ and $(m-1)(D_1 + D_2 + D_3 + D_4) + D_1 < 0$ and $m(D_1 + D_2 + D_3 + D_4) + D_1 > 0$, where $m \geqslant 1$ is an integer, then this branch of the stable manifold of the lower saddle point reaches the entrance saddle approach after circulating around all four heteroclinic orbits m times. The value of the energy at the entrance saddle approach is given by

$$\text{energy} = m(D_1 + D_2 + D_3 + D_4) + D_1.$$

Fig. 12 shows the case $m = 1$. For a given set of parameters D_i satisfying the foregoing constraints, the integer m can be expressed in the form:

$$m = 1 + \text{integer part of} \left[\frac{-D_1}{D_1 + D_2 + D_3 + D_4} \right] \tag{13}$$

or equivalently,

$$m = \text{integer part of}\left[\frac{D_2 + D_3 + D_4}{D_1 + D_2 + D_3 + D_4}\right]. \quad (14)$$

Note that as a parameter, say D_1, is varied, the topology of the resulting phase portrait changes at the points where

$$m(D_1 + D_2 + D_3 + D_4) + D_1 = 0, \quad m \geqslant 0. \quad (15)$$

At these special parameter values heteroclinic orbits occur (to the order of approximation of our analysis). That is, at these values the branch of the stable manifold of the lower saddle point that we are considering does not achieve the entrance saddle approach, but rather connects to the upper saddle point.

6.2. *Case II, continued: Second branch of the stable manifold of the lower saddle point*

We are now ready to consider the second branch of the stable manifold of the lower saddle point, that is, the branch which begins with the nearly heteroclinic orbit which we have denoted D_3. The analysis of the behavior of this branch is similar to that of the first branch of the stable manifold of the lower saddle point. This branch is not independent from the first branch of the lower saddle point as our calculations eventually will show. However, it is easier to proceed with the analysis of this branch by first ignoring any information concerning the other branch. Since $D_3 < 0$ and $D_3 + D_4 > 0$, this branch begins by following the orbits $D_3D_4D_1$. If $D_3 + D_4 + D_1 > 0$, this branch then reaches the entrance saddle approach, see Fig. 13.

However, $D_3 + D_4 + D_1$ is not necessarily positive. If $D_3 + D_4 + D_1 < 0$ this branch proceeds to follow in sequence orbits D_2, D_3, D_4 and then D_1 again. This conclusion is based on the following inequalities (being the energies at the next three saddle approaches): $D_3 + D_4 + D_1 + D_2 > 0$ from Eqs. (4) and (5); $(D_3 + D_4 + D_1) + (D_2 + D_3) < 0$ from Eq. (6) and the hypothesis $D_3 + D_4 + D_1 < 0$, $D_3 + D_4 + D_1 + D_2 + D_3 + D_4 > 0$ from Eqs. (4) and (5). Now on its final pass along D_1 it achieves the entrance saddle approach if $(D_3 + D_4 + D_1) + (D_2 + D_3 + D_4 + D_1) > 0$ (see Fig. 14), but it misses the entrance saddle approach and goes around again if $(D_3 + D_4 + D_1) + (D_2 + D_3 + D_4 + D_1) < 0$.

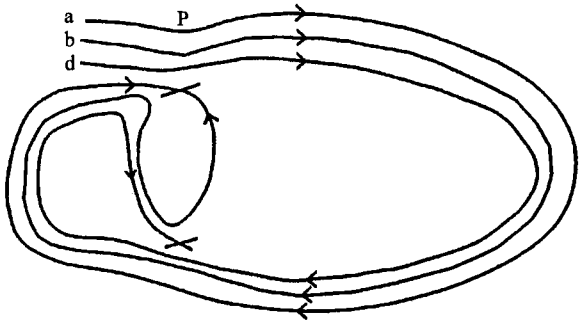

Fig. 13. Perturbed system, Case II: $D_2 > 0, D_3 < 0, D_4 > 0$, with $D_3 + D_4 + D_1 > 0$. The second branch of the lower saddle point, d, has been added to Fig. 10. Its energy at the entrance saddle approach P is $d = D_3 + D_4 + D_1$

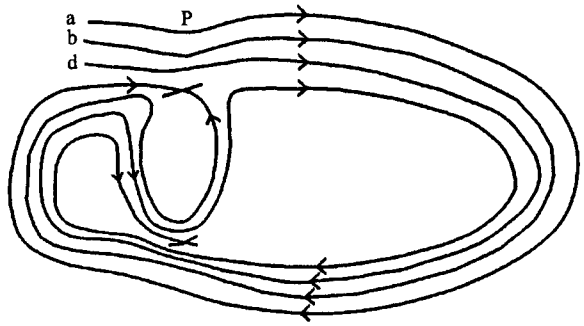

Fig. 14. Perturbed system, Case II: $D_2 > 0, D_3 < 0, D_4 > 0$, with $D_3 + D_4 + D_1 < 0$ but $(D_3 + D_4 + D_1) + (D_2 + D_3 + D_4 + D_1) > 0$. The second branch of the lower saddle point, d, has been added to Fig. 10. Its energy at the entrance saddle approach P is $d = (D_3 + D_4 + D_1) + (D_2 + D_3 + D_4 + D_1)$

As in the case of the first branch, this situation can be generalized as follows: If $D_3 + D_4 + D_1 < 0$ and $D_3 + D_4 + D_1 + (n-1)(D_2 + D_3 + D_4 + D_1) < 0$ and $D_3 + D_4 + D_1 + n(D_2 + D_3 + D_4 + D_1) > 0$, where $n \geqslant 1$ is an integer, then this branch of the stable manifold of the lower saddle point reaches the entrance saddle approach after circulating n times around $D_2 + D_3 + D_4 + D_1$, following the initial path of $D_3 + D_4 + D_1$. The value of the energy at the entrance saddle approach is given by

$$\text{energy} = D_3 + D_4 + D_1 + n(D_2 + D_3 + D_4 + D_1).$$

Fig. 14 shows the case $n = 1$. For a given set of parameters D_i satisfying the foregoing constraints, the integer n can be expressed in the form:

$$n = 1 + \text{integer part of}\left[\frac{-(D_3 + D_4 + D_1)}{D_1 + D_2 + D_3 + D_4}\right] \tag{16}$$

or equivalently,

$$n = \text{integer part of}\left[\frac{D_2}{D_1 + D_2 + D_3 + D_4}\right]. \tag{17}$$

Heteroclinic connections occur at the special parameter values:

$$D_3 + D_4 + D_1 + n(D_2 + D_3 + D_4 + D_1) = 0, \quad n \geqslant 0. \tag{18}$$

The countably infinite different topological sequences are caused by the heteroclinic orbits satisfying Eqs. (15) and (18). For example, for case II for arbitrary $D_4 > D_2 > 0$, the values of D_1 and D_3 may be chosen so that $D_1 + D_2$ and $D_3 + D_4$ are small and positive, in which case the number of loops will be large since $D_1 + D_2 + D_3 + D_4$ is small.

6.3. Case II, continued: Basins of attraction

The relative values of the number of loops (m and n) in the two branches of the stable manifold of the lower saddle point are constrained by the topology of the phase portrait. We rewrite Eq. (16) in the form:

$$n = 1 + \text{integer part of}\left[\frac{-D_1}{D_1 + D_2 + D_3 + D_4} - \frac{D_3 + D_4}{D_1 + D_2 + D_3 + D_4}\right] \tag{19}$$

and compare with the comparable expression for m, Eq. (13). Since

$$0 < \frac{D_3 + D_4}{D_1 + D_2 + D_3 + D_4} < 1 \tag{20}$$

we see that either $m = n$ or $m = n + 1$. More precisely,

$$m = n \quad \text{if} \frac{D_3 + D_4}{D_1 + D_2 + D_3 + D_4} < \text{fractional part of}\left[\frac{-D_1}{D_1 + D_2 + D_3 + D_4}\right]. \tag{21}$$

This may be written in an alternative form by noting that $-D_1/(D_1 + D_2 + D_3 + D_4)$ is the sum of its integer and fractional parts, and then using Eq. (13). The result is that

$$m = n \quad \text{if } m < \frac{D_2}{D_1 + D_2 + D_3 + D_4} \tag{22}$$

while

$$m = n + 1 \quad \text{if } m > \frac{D_2}{D_1 + D_2 + D_3 + D_4}, \tag{23}$$

where m is given by Eq. (13). The equivalent criterion for n is that

$$m = n \quad \text{if and only if } n > \frac{-D_1}{D_1 + D_2 + D_3 + D_4} \tag{24}$$

where n is given by Eq. (16). As examples of these cases, we sketch $m = n = 1$ in Fig. 15, and $m = 2$, $n = 1$ in Fig. 16. Note that Fig. 15 is a combination of Figs. 12 and 14.

We next discuss the basins of attraction of the three competing regions R, L and M. The four branches of the stable manifolds of the saddle points form the boundaries of the basins of attraction. In what follows we will discuss this for general m and n, but the reader may find it helpful to refer to Figs. 17 and 18 which display the basins of attraction, respectively, for the cases shown in Figs. 15 and 16, namely $m = n = 1$ and $m = 2$, $n = 1$.

The basins of attraction of the three regions R, L and M consist of four thin bands. In the case of $m = n$, the stable manifold of the lower saddle point splits the basins of attraction of R and L, while the stable manifold of the upper saddle point splits the basins of attraction of R and M. In addition, one branch of the unstable manifold of the upper saddle point splits the basin of attraction of R into two

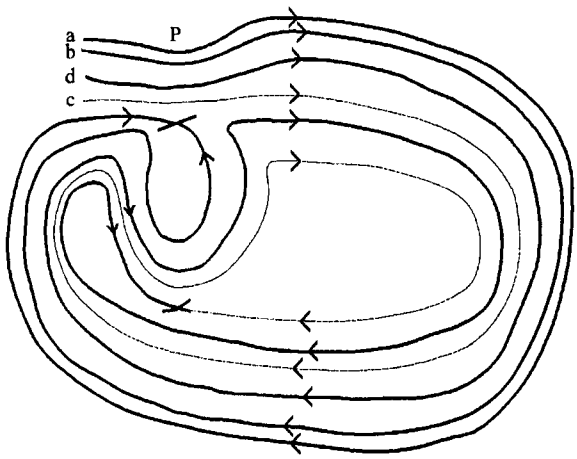

Fig. 15. Perturbed system, Case II: $D_2 > 0$, $D_3 < 0$, $D_4 > 0$, $m = 1, n = 1$. The first branch of the stable manifold of the lower saddle point is c (shown as lighter line), while the second branch is d. The energies at the entrance saddle approach P of the four branches of the stable manifolds are: $a = D_4 + D_1$, $b = D_1 + D_2 + D_3 + D_4$, $c = (D_1 + D_2 + D_3 + D_4) + D_1$, $d = (D_1 + D_2 + D_3 + D_4) + D_1 + D_3 + D_4$.

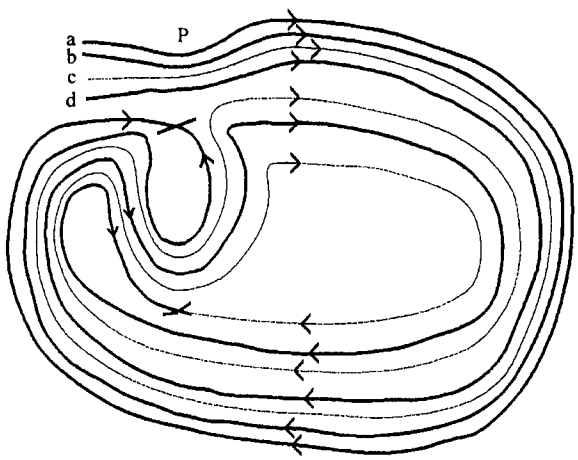

Fig. 16. Perturbed system, Case II: $D_2 > 0$, $D_3 < 0$, $D_4 > 0$, $m = 2, n = 1$. The first branch of the stable manifold of the lower saddle point is c (shown as lighter line), while the second branch is d. The energies at the entrance saddle approach P of the four branches of the stable manifolds are: $a = D_4 + D_1$, $b = D_1 + D_2 + D_3 + D_4$, $c = 2(D_1 + D_2 + D_3 + D_4) + D_1$, $d = (D_1 + D_2 + D_3 + D_4) + D_1 + D_3 + D_4$.

bands. See Figs. 15 and 17. The two R bands separate the L and M bands with the sequence $RLRM$ occurring at the entrance region.

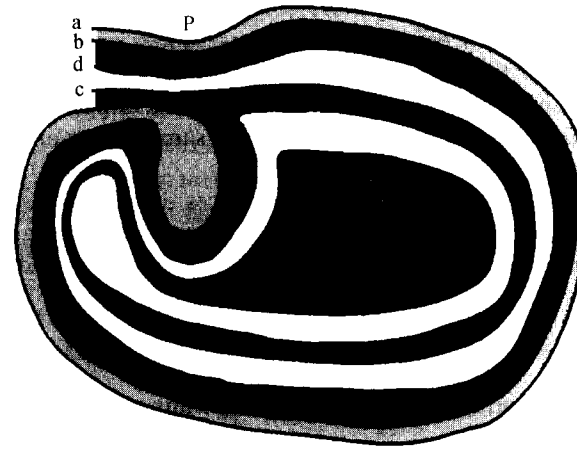

Fig. 17. Perturbed system, Case II: $D_2 > 0$, $D_3 < 0$, $D_4 > 0$, $m = 1, n = 1$. Basin of attraction of R is black, of L is white, and of M is shaded. Cf. Fig. 15.

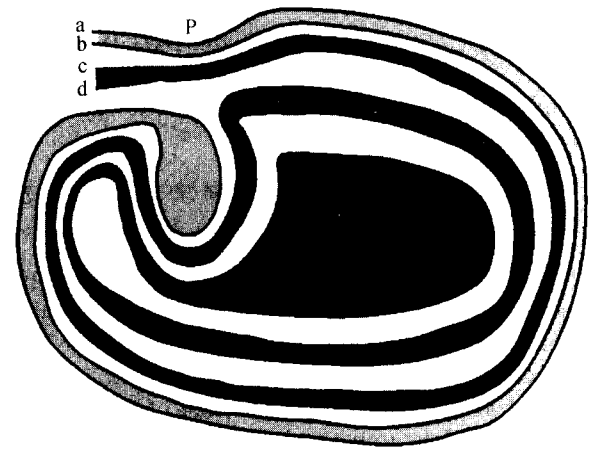

Fig. 18. Perturbed system, Case II: $D_2 > 0$, $D_3 < 0$, $D_4 > 0$, $m = 2, n = 1$. Basin of attraction of R is black, of L is white, and of M is shaded. Cf. Fig. 16.

In the case of $m = n$, if the energy at the entrance saddle approach of an inbound trajectory lies between 0 and $m(D_1 + D_2 + D_3 + D_4) + D_1$, then the motion enters R. If the energy lies between $m(D_1 + D_2 + D_3 + D_4) + D_1$ and $n(D_1 + D_2 + D_3 + D_4) + D_1 + D_3 + D_4$, then the motion enters L. If the energy lies between $n(D_1 + D_2 + D_3 + D_4) + D_1 + D_3 + D_4$ and $D_1 + D_2 + D_3 + D_4$, then the motion enters R. And if the energy lies

between $D_1 + D_2 + D_3 + D_4$ and $D_4 + D_1$, then the motion enters M. Using these values it is easy to show that the probability of capture does not depend on m and n nor on the particular topology of the band structure, and has the same values as in case I, Eqs. (9)–(11).

We now consider the sequences of orbits in the case $m = n$. The sequence of nearly heteroclinic orbits corresponding to capture into M has already been described

$$D_1D_4D_1D_4...D_1D_4 : D_1D_4D_3D_2D_3D_2D_3D_2D_3D_2....$$

The sequence of orbits corresponding to capture into L is

$$D_1D_4D_1D_4...D_1D_4 : D_1(D_4D_3D_2D_1)^nD_4D_3D_4D_3D_4D_3 ....$$

There are two bands corresponding to capture into R. The lower R band has the sequence

$$D_1D_4D_1D_4...D_1D_4 : (D_1D_4D_3D_2)^nD_1D_2D_1D_2D_1D_2...,$$

while the upper R band (which has one additional loop) has the sequence

$$D_1D_4D_1D_4...D_1D_4 : (D_1D_4D_3D_2)^{n+1}D_1D_2D_1D_2D_1D_2 ....$$

In the case of $m = n + 1$, the stable manifold of the lower saddle point again splits the basins of attraction of R and L, while the stable manifold of the upper saddle point splits the basins of attraction of L and M. In addition, one branch of the *unstable* manifold of the upper saddle point splits the basin of attraction of L into two bands. See Figs. 16 and 18. The two L bands separate the R and M bands with the sequence $LRLM$ occurring at the entrance region.

In the case of $m = n + 1$, if the energy at the entrance saddle approach of an inbound trajectory lies between 0 and $n(D_1 + D_2 + D_3 + D_4) + D_1 + D_3 + D_4$, then the motion enters L. If the energy lies between $n(D_1 + D_2 + D_3 + D_4) + D_1 + D_3 + D_4$ and $m(D_1 + D_2 + D_3 + D_4) + D_1$, then the motion enters R. If the energy lies between $m(D_1 + D_2 + D_3 + D_4) + D_1$ and $D_1 + D_2 + D_3 + D_4$, then the motion enters L. And if the energy lies between $D_1 + D_2 + D_3 + D_4$ and $D_4 + D_1$, then the motion enters M. Using these values it is again easy to show that the probability of capture has the same values as in case I, Eqs. (9)–(11).

We now consider the sequences of orbits in the case $m = n + 1$. The sequence of nearly heteroclinic orbits corresponding to capture into M is the same as in the case $m = n$:

$$D_1D_4D_1D_4...D_1D_4 : D_1D_4D_3D_2D_3D_2D_3D_2D_3D_2....$$

The sequence of orbits corresponding to capture into R is

$$D_1D_4D_1D_4...D_1D_4 : (D_1D_4D_3D_2)^mD_1D_2D_1D_2D_1D_2....$$

There are two bands corresponding to capture into L. The lower L band has the sequence

$$D_1D_4D_1D_4...D_1D_4 : D_1(D_4D_3D_2D_1)^nD_4D_3D_4D_3D_4D_3 ...,$$

while the upper L band (which has one additional loop) has the sequence

$$D_1D_4D_1D_4...D_1D_4 : D_1(D_4D_3D_2D_1)^{(n+1)}D_4D_3D_4D_3 D_4D_3....$$

7. Case III: Similar to case II

Case III is defined by $D_2 < 0$ and $D_3 > 0$. Eq. (4) requires that $D_1 > 0$. There is no restriction on the sign of D_4. If the phase portrait for case II is turned upside down (by rotation by 180°) it is seen that the same topology and flow direction is preserved. However, left and right become interchanged in this way so that $D_2 \Leftrightarrow D_3$ (D_2 is interchanged with D_3) and $D_1 \Leftrightarrow D_4$ (D_1 interchanged with D_4). In this way, case II becomes case III so that case III also has an infinite number of topological sequences, but these are related to case II by a rotation of 180°.

8. Discussion

In this work we assumed the perturbations to be autonomous, resulting in a two-dimensional

problem, cf. Eq. (1). Nevertheless we expect the basic topology considered here to be applicable to slowly forced problems, i.e. systems in which the perturbation is a function of slow time εt. Such a problem may be embedded in a three-dimensional space p-q-μ, where $\dot{\mu} = \varepsilon$. In this case the considerations discussed in this paper are expected to be applicable to the two-dimensional topology of a cross-section $\mu =$ constant. E.g. if the slow forcing were periodic then such a cross-section would be a Poincaré map. However, the forcing need not be periodic. The essential point is that the structures which correspond to the saddle points in this work must be normally hyperbolic motions [12].

A natural generalization of our results would be to a dynamical system with p saddles and $p + 1$ centers. If all $p + 1$ create stable attractors, then there would be $2p$ bands being attracted into the $p + 1$ stable attractors. Cases where some of the centers do not create a stable attractor can be analyzed in the same way.

References

[1] C.D. Hall, R.H. Rand, Spinup dynamics of axial dual-spin spacecraft, J. Guidance Control Dyn. 17 (1994) 30–37.

[2] C.D. Hall, Momentum transfer in torque-free gyrostats, Ch. 3, in: A. Guran (Ed.), Nonlinear Dynamics: The Richard Rand 50th Anniversary Volume, World Scientific Pub. Co., Singapore, 1997, pp. 60–88.

[3] R. Haberman, R. Rand, T. Yuster, Resonant capture for axial dual-spin spacecraft, Nonlinear Dynamics (1999) in press.

[4] B. Gladman, D.D. Quinn, P. Nicholson, R. Rand, Synchronous locking of tidally evolving satellites, Icarus 122 (1996) 166–192.

[5] D. Quinn, B. Gladman, P. Nicholson, R. Rand, Relaxation oscillations in tidally evolving satellites, Celestial Mech. Dyn. Astron. 67 (1997) 111–130.

[6] V.I. Arnold, Small denominators and problems of stability of motion in classical and celestial mechanics, Usp. Mat. Nauk 18 (1963) 91 [Russian Mat. Surveys 18 (1963) 85]

[7] A.I. Neishtadt, Probability phenomena due to separatrix crossing, Chaos 1 (1991) 42–48.

[8] A.V. Timofeev, On the constancy of an adiabatic invariant when the nature of the motion changes, Zh. Eksp. Teor. Fiz. 75 (1978) 1303–1308 (in Russian), Sov. Phys. JETP 48 (1978) 656–659.

[9] J.L. Tennyson, J.R. Cary, D.F. Escande, Change of the adiabatic invariant due to separatrix crossing, Phys. Rev. Lett. 56 (1986) 2117–2120.

[10] F.J. Bourland, R. Haberman, Separatrix crossing: time-invariant potentials with dissipation, SIAM J. Appl. Math. 50 (1990) 1716–1744.

[11] J. Guckenheimer, P. Holmes, Nonlinear Oscillations, Dynamical Systems, Bifurcations of Vector Fields, Springer, Berlin, 1983.

[12] D. Quinn, R. Rand, J. Bridge, The dynamics of resonant capture, Nonlinear Dyn. 8 (1995) 1–20.